Statistical n-Butyl Acrylate–Sulfopropyl Betaine Copolymers. 3. Domain Size Determination by Solid-State NMR Spectroscopy

Marc Ehrmann,† Jean-Claude Galin, and Bernard Meurer*

Institut Charles Sadron (CRM-EAHP), CNRS-ULP, 6 rue Boussingault, 67083 Strasbourg Cedex, France

Received February 10, 1992; Revised Manuscript Received October 29, 1992

ABSTRACT: The morphology of two statistical copolymers of n-butyl acrylate (A) and dimethyl(3-methacrylamidopropyl)(3-sulfopropyl)ammonium betaine (B) of B molar fraction 0.04 and 0.12 (copolymers AB-4.0 and AB-12) were analyzed through solid-state NMR spectroscopy (^{13}C CP/DD/MAS) over a broad temperature range (160–360 K). In spite of the complexity of molecular motions and carbon line overlapping, the measurement of selective hydrogen rotating frame spin-lattice relaxation time $T_{1\rho}$ through ^{13}C detection clearly shows that spin diffusion actually occurs over rigid microdomains of about 1 and 2.2 nm for the unclustered AB-4 and clustered AB-12 copolymers, respectively. These minimum dimensions, corresponding to the shortest path for magnetization relaxation, are likely characteristic of the zwitterionic multiplets which are the primary dipolar aggregates in these heterogeneous materials and are compatible with literature models relying on antiparallel alignment of the dipoles in close-packed structures.

Introduction

In the first two parts of this series we reported the synthesis[1] and the structural characterization[2] of statistical amorphous copolymers of n-butyl acrylate (A) and dimethyl(3-methacrylamidopropyl)(3-sulfopropyl)-ammonium betaine (B). In copolymers of low to moderate

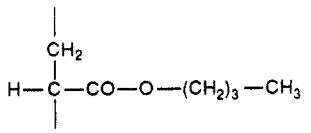

A

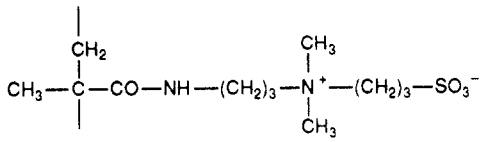

B

B content ($0.04 < F_B$ (molar content) < 0.35), strong specific dipolar interactions between zwitterionic units ($\mu \simeq 25$ D) result in a very typical biphasic structure characterized by two glass transitions in differential scanning calorimetry (DSC) related respectively to a soft matrix ($227 < T_g^S$ (K) < 253) containing only low amounts of B units ($F_B^S < 0.07$) and to hard domains ($303 < T_g^H$ (K) < 393) containing still rather high amounts of A units ($0.45 < F_A^H < 0.73$). Solid-state NMR (^1H wide line and ^{13}C high resolution) as a function of temperature and composition[2] confirmed the fair purity of a mobile phase and the strong chemical heterogeneity of a rigid phase. These are quantitatively correlated with the soft matrix and the hard domains identified in DSC.[2]

Moreover, small-angle X-ray scattering (SAXS) suggests a random distribution of heterogeneities within the polymeric matrix which still persist in the liquid state, far above the T_g^H of the hard domains. Rigid entities above T_g^H are also detected by ^1H wide-line NMR. Thus the multiphase morphology of these statistical copolymers may be considered as well ascertained, but a number of structural problems, quite typical in the field of ionomers[3,4] and zwitterionomers,[5] still remain to be quantitatively analyzed: shape, dimensions, and size distribution of the heterogeneities.

For the biphasic copolymers ($F_B > 0.04$), the presence of the "ionic peak" in the SAXS pattern does not allow one to derive reliable values of the dimensions of the scattering centers. The radius of gyration of about 1.4–2.0 nm previously reported[2] for a copolymer of low B content ($F_B = 0.04$) from a Guinier analysis of the SAXS profile at 433–453 K (temperature of vanishing of the ionic peak) would correspond to spherical units of 1.8–2.5-nm radius. On the other hand, the ^1H second moment M_2 of about 10 G^2 of the rigid phase[2] indicates strong spin–spin dipolar interactions which allow spin diffusion over these entities,[6] as confirmed by a single T_1 (^1H) >150 ms (60 MHz) and >300 ms (200 MHz). The minimum value of 150 ms reveals domain sizes less than 10 nm. Thus, the major goal of the present work is to probe the structure heterogeneity at a smaller scale by measuring spin diffusion in the millisecond range[6,7] with $T_{1\rho}(H)$. The wide chemical shift spread of the ^{13}C nuclei and the CP-MAS techniques[8] allow the selective detection of species involved in different dipolar environments.[9]

Two representative statistical AB copolymers (the figure following the symbol AB is related to the molar fraction of B units) were selected for extensive solid-state NMR measurements: "unclustered" sample AB-4.0, showing only one T_g at 233 K in DSC but exhibiting microphase separation according to ^1H NMR and SAXS analysis, and "clustered" sample AB-12, showing two glass transitions at 240 and 337 K. The former appears of definite interest as typical of borderline behavior; the latter, however, provides better signal to noise ratio in the ^{13}C NMR due to a greater amount of rigid phase.[2]

NMR Background

Numerous papers deal with applications of solid-state NMR to morphological investigations of heterogeneous structures,[6,10-15] relying on the short range of the magnetic dipole–dipole interactions. Because of energy-conserving flip-flops, magnetization can migrate on distances of some nanometers ($T_{1\rho}$) or tens of nanometers (T_1) in hard, i.e., near-rigid lattice domains (where magnetic interactions are not averaged by molecular motions).

In spite of impressive effort for the quantitative analysis of the spin diffusion mecanism,[14,15] a number of funda-

† Present address: Rhône-Poulenc Recherches, Centre de Recherches d'Aubervilliers, 93308-F Aubervilliers, France.

0024-9297/93/2226-0988$04.00/0

mental problems still remain to be solved. For the complex systems at hand, crude approximations[16] will be used for estimation of diffusion length:

$$\langle L^2 \rangle = D_s t_s$$

where D_s is the homonuclear H–H spin diffusion coefficient related to M_2 (1-nm diffusion length in 1 ms for M_2 = 20 G²)[7] and t_s is the diffusion time. $\langle L^2 \rangle^{1/2}$ is then the shortest path to a relaxation sink. During ^{1}H spin-lock, spin diffusion is slowed[6] down by a factor of 2.

We use resonant ^{1}H → ^{13}C magnetization transfer (cross polarization (CP)) for the selective detection of a carbon dipolar environment. The gain in selectivity is, however, severely hampered by loss in sensitivity, especially when the rigid fraction is small, such as in the case of copolymers of low zwitterionic content. Therefore, no attempt will be made to analyze the cross-polarization rates as experimentally determined, although spectra are distinctively different at different contact times.

In contrast to literature results on well-organized heterogeneous systems,[17] quantitative correlation of the fractions of given mobility as derived from ^{1}H wide line shape analysis[2] (rigid, intermediate, and mobile components) with morphology as revealed by CP dynamics appears hazardous for the investigated systems: if the magnetization transfer rate T_{CP} depends strongly on dipolar heteronuclear interactions within distances of 1–5 Å, the enhancement factors vary also with the whole carbon dipolar environment.[18,19]

^{13}C magnetization evolution during CP is described by the following equation:[18,19]

$$S = S_0 T_{CP}^{-1}\{T_{CP}^{-1} + T_{1\rho}(C)^{-1} - T_{1\rho}(H)^{-1}\}^{-1}\{\exp[-t/T_{1\rho}(H)] - \exp[-t(1/T_{CP} + 1/T_{1\rho}(C))]\}$$

where S_0 is the Hartmann–Hahn maximum ^{13}C magnetization, T_{CP} is the characteristic time of the heteronuclear magnetization transfer, $T_{1\rho}(C)$ is the component of the rotating frame spin–lattice $T_{1\rho}$ of carbons under ^{1}H decoupling, and t is the contact duration.

With the usual assumption $T_{1\rho}(C) \gg T_{CP}$, this simplifies to

$$S_1 = S_0\{1 - T_{CP}/T_{1\rho}(H)\}^{-1}\{\exp[-t/T_{1\rho}(H)] - \exp[-t/T_{CP}]\}$$

i.e., magnetization grows exponentially with the T_{CP} time constant and decays exponentially with $T_{1\rho}(H)$.

The CP signal after a ^{1}H spin-lock of duration τ follows

$$S_2 = S \exp[-\tau/T_{1\rho}(H)]$$

In heterogeneous multiphase materials, the spin–lattice relaxation in the rotating frame is often distributed.

Experimental Section

Materials. The synthesis and characterization of the A_n and B_n homopolymers and AB copolymers were previously described.[1] The copolymers showed good chemical homogeneity, and molecular weights M_w were in the range (1.1–2.6) × 10⁵. Poly[((dimethylamino)propyl)methacrylamide] (B'_n) was obtained by standard free radical polymerization in dioxane solution.

All of the samples were dried at 80 °C under 1.3 Pa for 24 h before experiments and handled under N_2 gas. Possible residual water was not a problem in our measurements.

NMR Techniques. Experiments were performed on a Bruker CXP 200 spectrometer (^{1}H resonance at 200 MHz, ^{13}C resonance at 50.3 MHz). A Bruker VT-MAS 7-mm probe with a zirconia rotor allowed 1–2-kHz magic angle sample spinning (MAS) in the 160–360 K temperature range. Accurate adjustment of rotation angle at $\cos^{-1}(1/\sqrt{3})$ was performed on KBr. The long measuring time (typically 24 h for one relaxation curve) implied constraints on the spinner operation: (i) The driving and bearing gas was provided by evaporating liquid N_2 at 7 bars from a vessel of 160 L (Cryodiffusion EMP 160), giving 3–4 days of continuous operation. (ii) The cooling of the bearing gas was achieved by a heat exchanger immersed in liquid N_2 (Dewar of 25 L). The N_2 consumption was monitored by weight watching, and refilling was done on-line from a 100-L storage tank every 6–12 h, depending on the temperature.

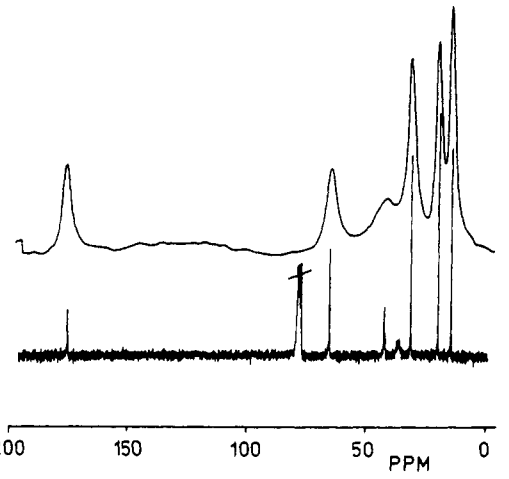

Figure 1. ^{13}C high-resolution spectra of sample A_n in solution (bottom) and of the mobile component from SPE (top) on sample AB-4.0.

We used 4-μs 90° pulses, i.e., 40-kHz ^{1}H and ^{13}C radiofrequency field strengths.

^{13}C spectra of the mobile fraction were recorded with single pulse excitation (Bloch decay), ^{1}H high-power decoupling, and MAS(SPE).[8] Standard pulse sequences[8] were used for CP-MAS spectra, while selective $T_{1\rho}(H)$ were measured by ^{1}H spin-locking followed by CP and dipolar decoupling.[9] Phase cycling and add–subtract were systematical.

Due to the low signal to noise ratio, statistical analysis of the data was mandatory. It was performed on an IBM-PC with the ASYST language (peak integration, curve fitting by nonlinear iterative least squares minimization).

^{13}C solution spectra were recorded on Bruker AC 200 and AM 400 spectrometers at room temperature and with broad-band MLEV ^{1}H decoupling. Solvents depended on the polymer under investigation: $CDCl_3$ for A_n, D_2O for B'_n and B_n, and trifluoroethanol (TFE) for B_n and AB copolymers.

Results

^{13}C Chemical Shift Assignments. The analysis of the copolymer spectra requires previous assignments of the lines of the parent homopolymers.

The chemical shifts of A_n carbons are already known[20,21] (Figure 1). The assignment of the B_n lines was carried out using the solution spectra of its tertiary amino polymeric precursor B'_n, of the zwitterionic model compound triethyl(sulfopropyl)ammonium betaine[22] and DEPT measurements (Table I).

Note that carbonyl, quaternary, and α-methyl carbons are split by configurational effects and so easily recognizable. The tertiary amine quaternization induces chemical shifts for C2, C3, and C4. In the spectrum shown Figure 2B, the pattern of the AB-12.0 copolymer is quite well the superposition of those of the parent homopolymers. The carbonyl is sensitive to neighboring units.[1] The zwitterionic carbons are readily apparent in the solid-state CP-MAS spectrum (Figure 2A).

Cross-Polarization Dynamics. The CP-MAS spectra show all of the lines of the B_n solution spectrum at contact times of 100–400 μs and mostly the lines of A_n at longer contact times of 1–5 ms (see Figure 3).

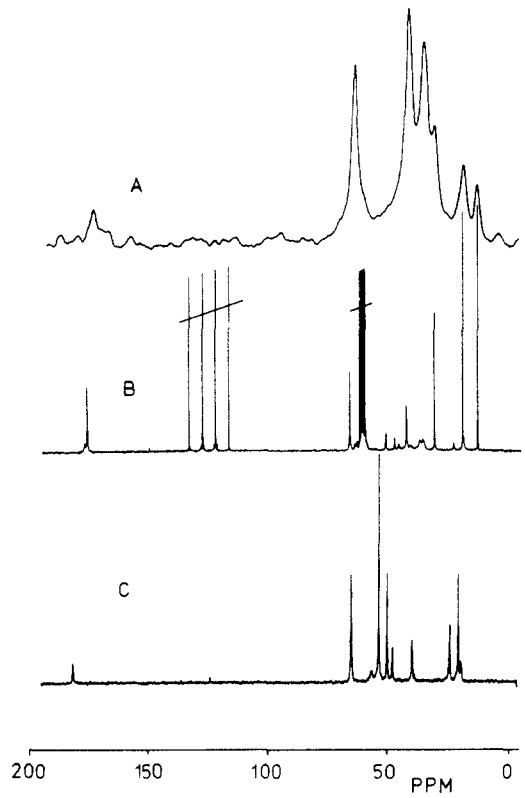

Figure 2. ^{13}C high-resolution spectra: solid-state CP-MAS spectrum of AB-12.0 at 360 K with a contact time t_{CP} = 600 μs (A); solution spectra at 300 K for sample AB-12.0 (B) and B_n (C).

Table I
^{13}C Line Assignments (Shifts in ppm from TMS)

		B_n		AB-12.0 (TFE)	
carbon	B'_n D_2O	D_2O	TFE	A	B
Cq	49	48.0	47.3	41.5	47.4
Cα	20	20.2			20
Cβ	57	56.4		35.4, 36.3	59
CO	182	181.8	179.2	174.5	176.6
C1	41	39.1	37	64.4	41
C2	28	24.4	22.4	30.7	23.0
C3	59	65.1		19.1	63 ● 0.5
C4	47	53.6	51.3	13.7	50.9
C5		65.1			63 ± 0.5
C6		21.1	17.3		18.8
C7		50.2	46		46

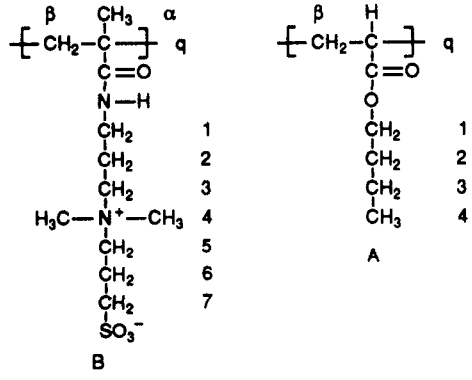

There is an ambiguity on this two-step behavior: the longer T_{CP} of A units can originate either from some mobility leading to reduced dipolar interactions even for the units incorporated in ionic aggregates (and) or from the magnetization of the acrylate carbons by ^1H spin diffusion to the interface between hard domains and the mobile surroundings. From preceding studies,[2] we know that A units remain incorporated in rigid domains observed

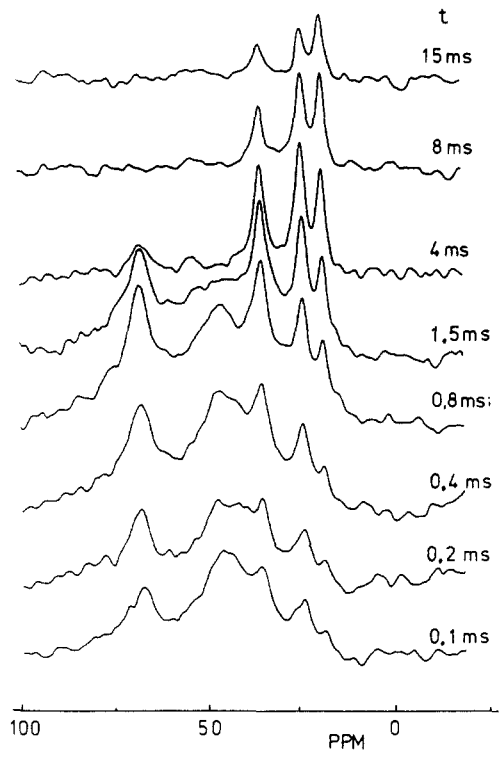

Figure 3. CP-MAS spectra as a function of contact time t_{CP} for AB-4.0 at 300 K (1000 scans, 3-s recycling).

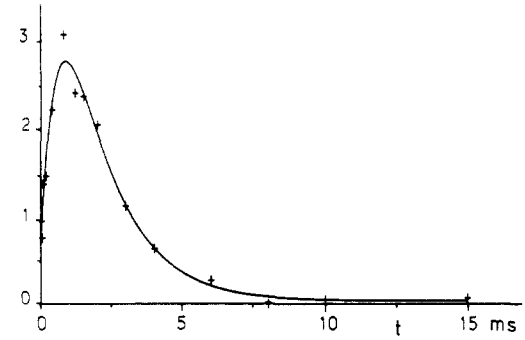

Figure 4. Intensity of line at 63.6 ± 2 ppm as a function of contact duration (same conditions as in Figure 3). The solid line is a best fit of two exponentials (five parameters) according to $M(t) = 0.011 + \exp(-t/1.6\ \text{ms}) - \exp(-t/0.60\ \text{ms})$.

at low frequency (from the very low frequency of DSC to ca. 10 kHz by ^1H NMR) at temperatures above the lower T_g so that both effects take place at the time scale of cross-polarization.

In all cases, numerical analysis of standard cross-polarization dynamics will be difficult because of the carbon line overlapping in the spectra due to the solid-state line width of the glassy compounds; signal evolution involves at least two time constants for the growth and two for the decay. Such an analysis is outside the experimental accuracy, and at most three time constants (for example, two for the growth and one for the decay) amounting to seven parameters were statistically adjusted, delaying the determination of the decay constants $T_{1\rho}(H)$ to a direct measurement performed in a second stage.

With these assumptions (see the example in Figure 4), results of growth and decay rates of signal intensity as a function of contact times for sample AB-4.0 are given in Table II. The decay in cross-polarization is clearly not only due to $T_{1\rho}(H)$ but involves a nonnegligible contribution of $T_{1\rho}(^{13}C)^D$ arising from some molecular motions.[8] This complexity is best seen for sample AB-12: the data obtained are difficult to analyze because of line overlap

Table II
Time Constants (ms) for Growth (T_{CP}) and Decay (Labeled $T_{1\rho}$(H)) of CP Magnetization on Sample AB-4.0

	300 K		250 K		220 K		200 K	
spectral region (ppm)	T_{CP}	$T_{1\rho}$(H)	T_{CP}	$T_{1\rho}$(H)	T_{CP}	$T_{1\rho}$(H)	T_{CP}	$T_{1\rho}$(H)
13.7 ± 2	1.05	17.6	0.20	4.8	2	0.5 (10%) 4 (90%)	0.62 4.9	6.6
19.1 ± 2	0.70	1.1 (28%) 15.3 (72%)	0.17	3.7			0.15 1.5	5 10
36.6 ± 2	0.42	4.1	0.08	4.3	1.5 4.5	6.5		
42.2 ± 4	0.27	1.9	0.30 (50%) 1.70 (50%)	3	1.5 4.4	6.8		
63.6 ± 4	0.6 (56%) 1.6 (44%)	1.6	0.21	1.7	3	7		

Table III
$T_{1\rho}$(H) Values for Sample AB-4.0[a]

spectral region (ppm)	160 K	180 K	200 K	220 K	250 K	270 K	300 K	320 K	340 K	360 K
13.7 ± 2	1.52 (d)	1.98 (d)	4.3 (a) 5.5 (e)	6.2 (a) 3.2 (e)	0.93 (a)	0.78 (b)	2.4 (e)	1.3 (c)	2.3 (c)	9.3 (c)
19.1 ± 2	1.85 (d)	2.40 (d)	4.7 (a) 5.8 (e)	6.0 (a) 3.4 (e)	0.91 (a)	0.53 (b)	1.94 (e)	0.93 (c)	2.0 (c)	4.3 (c)
36.6 ± 2	1.92 (d)	2.37 (d)	5.2 (a) 5.9 (e)	6.2 (a) 3.5 (e)	0.96 (a)	0.48 (b)	1.33 (e)	0.70 (c)	1.6 (c)	2.5 (c)
42.2 ± 4	2.07 (d)	2.37 (d)	5.2 (a) 6.0 (e)	6.6 (a) 3.6 (e)	1.01 (a)	0.57 (b)	0.90 (e)	0.65 (c)	3.3 (c)	2.4 (c)
63.6 ± 4	2.34 (d)	4.74 (d)	5.2 (a) 4.9 (e)	5.8 (a)	1.52 (a)	≃0.25 ±0.01 (b)				

[a] Contact time value (T_{CP}) of (a) 400 μs, (b) 500 μs, (c) 600 μs, (d) 1 ms, and (e) 2 ms.

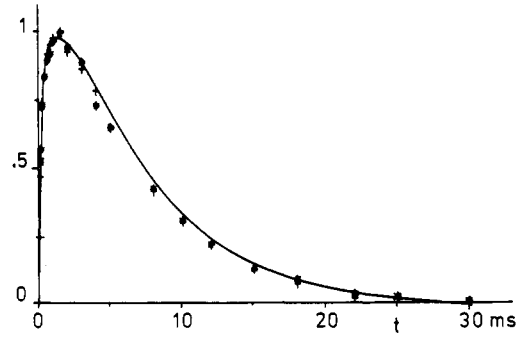

Figure 5. Intensity of lines at 13.7 ± 2 (+) and 19.1 ± 2 pmm (*) as a function of contact time on sample AB-12.0 at 200 K. The solid line is operator best-fit with growth constants of 0.18 and 2 ms and decay constants of 9 and 17 ms.

and strong C–H dipolar interactions giving individual T_{CP} as exemplified Figure 5.

T_1(H) Measurements. The hydrogen spin–lattice relaxation of samples AB-4.0 and AB-12 measured at 60 and 200 MHz are (mono)exponential in the investigated temperature range. T_1(H) at 60 MHz increases from a broad minimum of 170 ms at 190 K to 250 ms at 300 K. T_1(H) at 200 MHz increases from 320 to 550 ms in the same temperature range. The ratio of ca. 2 of relaxation times at the two the magnetic fields points to spin diffusion for controlling relaxation rates.

$T_{1\rho}$(H) Measurements. The $T_{1\rho}$(H)'s of sample AB-4.0 (Table III) show that spin diffusion becomes efficient for equalizing relaxation rates below 200 K only for the spectral pattern between 17 and 50 ppm. Outside this temperature window, the $T_{1\rho}$(H) values depend on the CP duration and are not exponential.

The $T_{1\rho}$(H) temperature variations of sample AB-12 are drawn Figure 6. From 190 to 250 K, spin diffusion is suggested by the similarity of the spectra recorded by varying the spin-lock duration τ prior to ^{13}C detection (Figure 7). Spin diffusion is actually operative as revealed by a (mono)exponential decay (Figure 8). Full 2D experiments along delay τ and contact duration t cannot be performed on the old ASPECT 2000 computer at hand due to memory and disk space limitations.

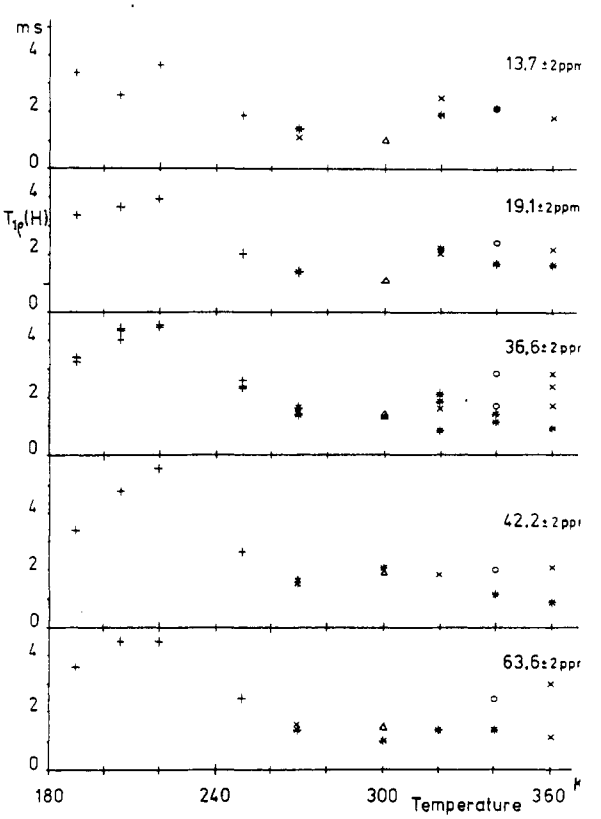

Figure 6. Temperature variation of selected $T_{1\rho}$(H) for sample AB-12.0. Each point is determined by 20–30 delayed spectra of 1000 scans. Contact time of 0.4 (*), 0.8 (△), 1 (+), 2 (×), and 3 ms (○).

Discussion

The spread of T_1(H) and $T_{1\rho}$(H) minima over a temperature range of 50 K is indicative of a distribution of correlation times. This does not allow discussion of

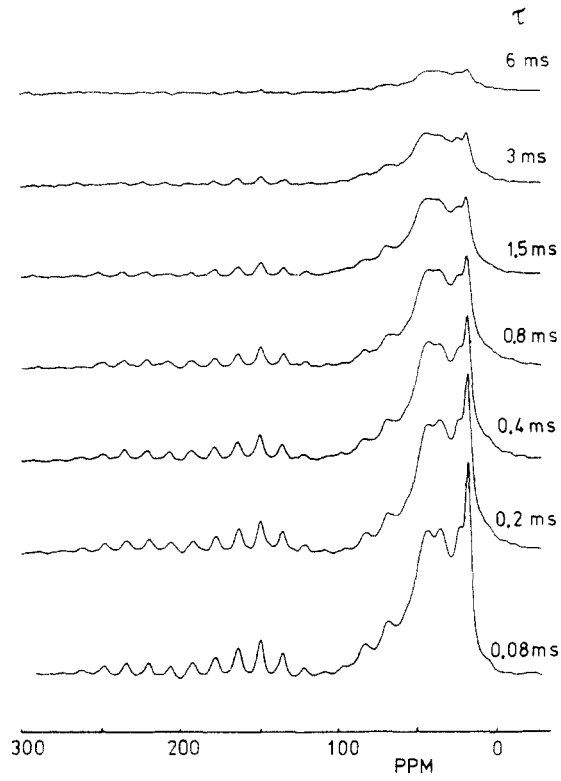

Figure 7. Selective ^{13}C detection of $T_{1\rho}(H)$ for sample AB-12.0 at 190 K with a contact time of 1 ms. Each spectrum results from 1000 scans at a 5-s repetition time.

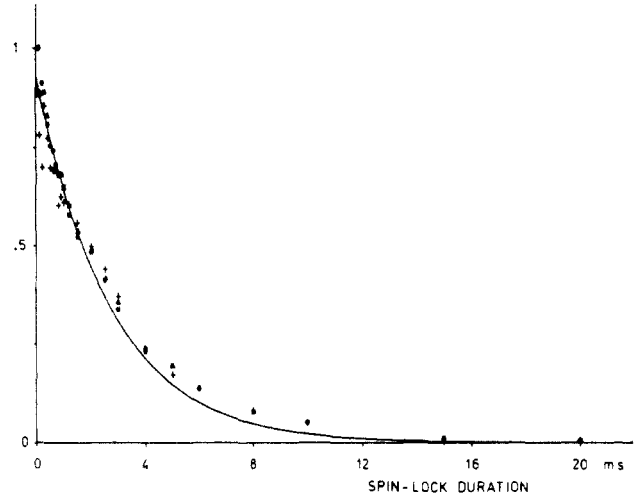

Figure 8. $T_{1\rho}(H)$ measured (same sample and conditions as in Figure 7) by integration of spectral regions ((+) 63.2 ± 2, (Δ) 38.0 ± 2, and (*) 30.2 ± 2 ppm) and exponential fitting which indicates a unique $T_{1\rho}(H)$ of 2.65 ± 0.2 ms.

molecular motions in terms of correlation times and activation energies as manifested through T_2 or $T_{1\rho}(^{13}C)$, in contrast to the proposed behavior for the homopolymer A_n.[19,20] For the complex materials under study, the multicomponent wide lines[2] preclude a difficult $T_{1\rho}(H)$ component analysis (i.e., analysis of the distribution of time constants in terms of a sum of exponentials), even measured directly on the more sensitive H channel.

At temperatures above T_g, the spin–lattice relaxation is likely controlled by the ammonium methyl groups, which provide efficient relaxation sinks with very short spin-diffusion paths. At lower temperatures, the uniqueness of the relaxation rate points to spin diffusion over longer distances.

Assuming in a first approximation that spin diffusion occurs in a continous three-dimensional space, the minimum size of the corresponding rigid microdomains may be calculated to be about 1 and 2.2 nm for sample AB-4.0 at 160 K and sample AB-12 at 200 K, respectively. These distances are high enough to be compatible with the a priori assumed 3D continuous model. The second-moment constancy[2] of the rigid phase in this temperature range supports the validity[6] of the approach.

The significant increase of the diffusion length with zwitterion content may be ascribed to a corresponding increase of the aggregation number and of the size of the dipolar aggregates. These estimated dimensions may be critically compared with some data related to similar systems.

According to molecular mechanics computation,[23] low molecular weight model compounds such as *n*-hexyldimethyl(sulfopropyl)ammonium betaine are likely packed in platelets, disks, or tubes, allowing antiparallel alignment of their dipolar heads in an extended conformation (μ = 27.7 D, corresponding to a charge-to-charge distance of 0.58 nm). Spherical structures are never energetically favorable. Semitelechelic polyisoprenes of low molecular weight (M_w < 4700) bearing one identical zwitterionic end group[24] show long-range order corresponding to a triangular array of cylinders of 1.3-nm diameter (hard core of interacting zwitterions). It is worth emphasizing that these models cannot be directly transposed to the statistical copolymers under study since the microenvironment of the interacting zwitterionic units is strongly different: the backbone and the neighboring units result in drastically higher steric hindrance with respect to an end group. Moreover, B units are not exclusively located as isolated units in AB*A triads: even for copolymers of low B content, because of very different reactivity ratios of the two monomers[1] (r_A = 0.42 and r_B = 6.0), the fractions of B units in AB*B and BB*B triads are 0.17 and 0.01 for copolymer AB-4.0 and 0.37 and 0.06 for copolymer AB-12.0. All of these features do not allow any reliable a priori assumption on the shape and the size of the zwitterionic aggregates, which may also show some polydispersity in aggregation number.

In any case, the diffusion distances of a few nanometers as derived from solid-state NMR spectroscopy are compatible with the radius of gyration of about 1.4–1.9 nm of the scattering entities derived from SAXS analysis on copolymer AB-4.0 between 433 and 483 K.[2] They are still compatible with the dimensions of the other sulfopropyl betaine aggregates measured on the semitechelic polyisoprenes (see above) or calculated for some model aggregates (see, for instance, the more stable "lateral" configuration of a tetramer of *n*-hexyldimethyl(sulfopropyl)ammonium betaine associating two dimers side by side over thickness higher than 1 nm[24]).

Conclusion

In spite of a number of unavoidable drawbacks (complexity of solid-state NMR spectra and molecular motions), probing spin diffusion provides a reliable estimate of the dimensions of the rigid aggregates characteristic of the zwitterionomers under study. The NMR spectroscopy clearly tests the material at a very local scale and thus likely focuses on the B-rich multiplets which are the primary aggregates in these complex heterogeneous materials, without significant sensitivity to their possible packing within clusters previously identified by DSC measurements.[2] Optimization of the NMR techniques would allow a better characterization of the rigid multiplets still present at temperatures far above the higher T_g for clustered copolymers such as AB-12.[2] However, a truly

quantitative structural description of the zwitterionomers in terms of shape, size, polydispersity, and distribution of these heterogeneities still remains a challenge. Finally, a more regular distribution of the dipolar interacting units along the macromolecular chain, such as in some segmented poly(ionenes) described in the literature,[25,26] would probably result in a better defined multiplet structure and potential long-range order in these zwitterionomers.

Acknowledgment. The authors gratefully acknowledge Rhône-Poulenc for a grant to M.E.

References and Notes

(1) Ehrmann, M.; Galin, J. C. *Polymer* **1992**, *33*, 859.
(2) Ehrmann, M.; Mathis, A.; Meurer, B.; Scheer, M.; Galin, J. C. *Macromolecules* **1992**, *25*, 2253.
(3) Eisenberg, A.; Hird, B.; Moore, R. B. *Macromolecules* **1990**, *23*, 4098.
(4) Mauritz, A. K. *J. Macromol. Phys.* **1988**, *C28*, 65.
(5) Salamone, J. C.; Rice, W. C. *Encyclopedia of Polymer Science*; Wiley-Interscience: New York, 1988; Vol. 11.
(6) VanderHart, D. L. *Makromol. Chem., Macromol. Symp.* **1990**, *34*, 125.
(7) McBrierty, V. J.; Douglass, D. C. *J. Polym. Sci., Macromol. Rev.* **1981**, *16*, 295.
(8) Komoroski, R. A. High Resolution NMR Spectroscopy of Synthetic Polymers in Bulk. In *Methods in Stereochemical Analysis*; VCH Publishers: Deerfield Beach, FL, 1986; Vol. 7.
(9) Stejskal, E. O.; Schaefer, J.; Sefcik, M. D.; McKay, R. A. *Macromolecules* **1981**, *14*, 275.
(10) McBrierty, V. J.; Douglass, D. C.; Kwei, T. K. *Macromolecules* **1978**, *11*, 1265.
(11) Tekely, P.; Laupretre, F.; Monnerie, L. *Polymer* **1985**, *26*, 1081.
(12) Schenk, W.; Reichert, D.; Schneider, H. *Polymer* **1990**, *31*, 329.
(13) Schaefer, J.; Garbow, J. R.; Stejskal, E. O.; Lefelar, J. A. *Macromolecules* **1987**, *20*, 1271.
(14) Havens, J. R.; VanderHart, D. L *Macromolecules* **1985**, *18*, 1663.
(15) Schmidt-Rohr, K.; Spiess, H. W. *Macromolecules* **1991**, *24*, 5288.
(16) Abragham, A. *Principles of Nuclear Magnetism*; Clarendon Press: Oxford, 1961.
(17) Tanaka, H.; Nishi, T. *Phys. Rev. B* **1986**, *33*, 32.
(18) Mehring, M. *Principles of High Resolution NMR in Solids*: Springer: Berlin, 1983.
(19) Voelkel, R. *Angew, Chem., Int. Ed. Engl.* **1988**, *27*, 1468.
(20) Voelkel, R. *Polym. Prepr. (Am. Chem. Soc., Div. Polym. Chem.)* **1988**, *29*, 52.
(21) Llaura Darricades, M. F.; Pichot, C.; Guillot, J.; Rios, L. G.; Cruz, M. A. E.; Guzman, C. C. *Polymer* **1986**, *27*, 889.
(22) Zicmanis, A.; Zilniece, I.; Uzijs, H. *Latv. PSR Zinat. Akad. Vostis, Kim. Ser.* **1979**, *5*, 605.
(23) Bredas, J. L.; Chance, R. R.; Silbey, R. *Macromolecules* **1988**, *21*, 1633.
(24) Shen, Y.; Safinya, C. R.; Fetters, L.; Adam, M.; Witter, T. *Phys. Rev. A* **1991**, *43*, 1886.
(25) Feng, D.; Venkateshwaran, L. N.; Wilkes, G. L.; Meir, C. V. M.; Stark, J. E. *J. Appl. Polym. Sci.* **1989**, *37*, 1549.
(26) Feng, D.; Wilkes, G. L.; Leir, C. M.; Stark, J. E.; *J. Macromol. Sci., Chem.* **1989**, *A26*, 1151.